Effects of temperature on fluid lubricant consistency under adiabatic cylindrical rolling boundaries

Jalatheeswari N*
Dept.of Mathematics,KMCPGS, Lawspet, Puducherry, India
njalatheeswari@gmail.com

Dhaneshwar Prasad
Dept.of Mathematics,KMCPGS, Lawspet, Puducherry, India
rpdhaneshwar@gmail.com
* author for correspondence

Abstract: **In this paper, the rigid cylindrical rollers, with rolling and normal squeezing motions, lubricated by a power law fluid are studied under the adiabatic boundary conditions. The consistency of the lubricant assumed to vary exponentially with pressure and mean temperature. By solving the modified Reynolds and Heat equations simultaneously to get pressures and temperatures. Different characteristics of roller bearings are analyzed and discussed. A non- uniform grid was employed to achieve more accurate predictions of pressure and temperature, especially in the high pressure region. The detailed analyze of the theoretical results obtained herein seems to suggest that the temperature dependence of the lubricant viscosity causes a reduction in both the load carrying capacity and surface traction of the system , whereas the normal squeezing motion leads to a substantial increase in pressure and also displaces the pressure peak towards the centre line of contact. Also results are compared with previous findings.**

Keywords: Cylindrical Roller, non-Newtonian, lubrication, squeezing velocity, pressure, mean temperature, lubricant consistency, load, traction.

I. INTRODUCTION

Machines have made our life a sophisticated one. Modernism has absolutely changed our life style. Along with machines, man too work twenty-four hours on shift basis. Like our physique, the machine too emit heat at work. Rest is the remedy to man but machines demand lubricant as remedy. Lubrication maximizes the life of the roller bearing. Dowson[1] was pioneer to propose a bond between relative film thickness and the capacity of the contacting surface to tolerate pitting. The efforts to propose Sigmoid curve by Lin et al.[2] was experimentally demonstrated by Skurka[3] and Danner[4].

In the beginning, grease was used as lubricant without oil circulation system and filtering. Wilson[5] proposed experiments for roller bearing via electrical capacitance measurements. He calculated film thickness to radially loaded double row spherical roller and single-row cylindrical roller. Later, "Lubcheck" device for surveying lubrication was delivered by Heemskerk et al[6]. This method was also relied upon electrical capacitance measurement. The probability of asperity contacts was calculated by using grease or oil in radially loaded deep-groove bell bearing. Later, the same device was used by Leenders and Houpert[7] and Wikstrom and Jackobson for spherically roller bearings. Wardle et al.[8] and Jacobson used the same Lubcheck apparatus to experiment with refrigerant-lubricant mixture and Masen et al.[9] used it intwo-disc test rig to study surface micro-geometry on film formation.

Franke and Poll [10] exploited the capacitance technique to assess the speed, temperature and friction torque of the lubrication condition. This test was conducted using angular contact ball bearings with ten test grease lubrication. The lubrication in ball-on-flat and the lubrication in roller bearing is not similar. In roller bearing the lubricant flows fully inside the bearing. The level of starvation, the contact area geometry, and the dynamics of the rollers and cage, all has reasonable effect upon the film thickness. This is not possible in ball and disc model (Lugt [11]). Murer et al. [12] studied the load distribution in roller bearing using electrical capacitance. Schnabel and company [13] delivered that in mixed regime the character of contact capacitance is not clear. And it has to be augmented to know the additives play in impedance measurement. Recently, Jablonka et al.[14] used chromiumcoated glass disc to assess the lubricant film thickness via optical interferometry and electrical capacitance. He experimented with 7 steel balls. Six ceramic balls(silicon nitrate) replaced the six steel balls. Because of the non-conductive character of silicon nitrate, the obtained figure responds to the film thickness between the steel balls and the rings.

A known fact is that lubricant failure is the primary cause of the failure of the bearing. Further, it is hard to calculate the life and properties of the fresh grease. The ageing can be classified both in terms of mechanical and chemical. It is quite natural to witness physical and chemical changes at high temperature operation due to mechanical and thermal stress. The way these changes affect the film is not clear. Still it is said that bearings fail at the cause of lubrication failure rather than surface fatigue [15]

Dowson[16] demonstrated that film thickness has a direct effect on steady-state wear rare for metal-on-metal joints tested in a hip joint simulator. When the film thickness increases the steady-state wear rate decreases in magnitude. Though the correlation is surprising, the strongest correlation would be with the lambda ratio provided the phenomenon is credited to asperity interactions. It is learnt that modern production techniques make sure that after bedding-in roughness and the surface form of several implants show same result, regardless of diameter, material design and clearance.

Cann [17] considered on the ball on disc test rig to bring relationship between starved film thickness and different temperatures. To study the above said point he used lithium grease. It was realized that film thickness decreased faster at high speed. At the same time reflow was stronger at lower speed and higher temperature. Further Cann[18] discovered that starvation was more when lithium grease of high thickener concentration and base oil viscosity was used. Hurley et al.[19] from his studies suggested that thermally aged and heavily aged lithium grease gave higher film thickness. Couronne et al.[20] tested 4 different grease using a ball on disc and showed 2 out of 4 lubricant showed increase and then decrease in film thickness.

In this present paper analysis is fully focused to examine the qualitative behavior of thermal effects on non-Newtonian power law lubrication of two heavily loaded rigid cylindrical roller bearings underneath adiabatic and isothermal boundaries. The lubricant consistency variation assumed to vary along with the pressure and the mean film temperature. The rolling ratio are used to study the rolling/ sliding effects of surfaces on the pressure, the temperature and the lubricant consistency along with load and traction. however, the effects of compressibility and surface roughness are neglected.

II. MATHEMATICAL ANALYSIS

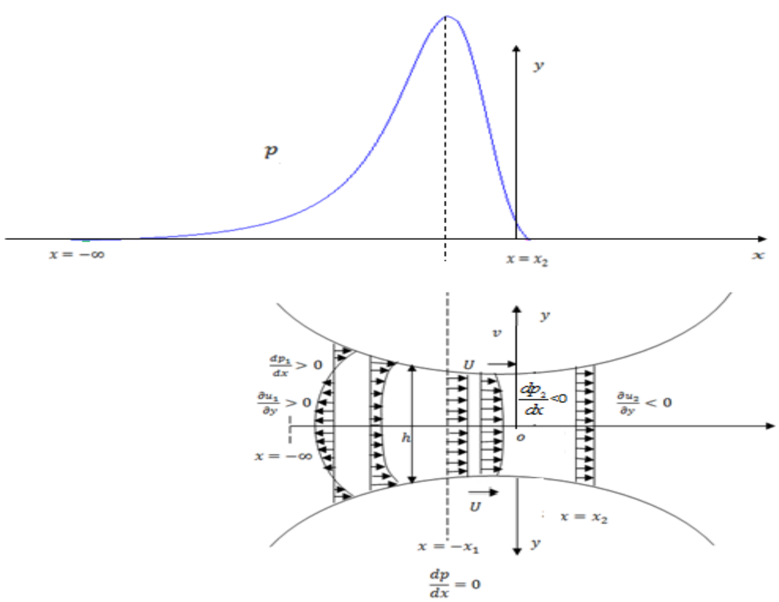

Fig 1: Lubrication of cylindrical rollers

The governing equations for the one dimensional fluid flow are [21]

$$\frac{dp}{dx} = \frac{\partial \tau}{\partial y}. \quad (1)$$

$$\frac{\partial u}{\partial x} + \frac{\partial v}{\partial y} = 0. \quad (2)$$

Where the shear stress relation for this case is

$$\tau = m\left|\frac{\partial u}{\partial y}\right|^{n-1}\frac{\partial u}{\partial y}. \quad (3)$$

The consistency m of the above power- law is taken as:

$$m = m_0 e^{\alpha p + \left(\frac{T_0}{T_m}\right)}. \quad (4)$$

Where the mean temperature T_m is defined as

$$T_m = \frac{2}{h}\int_0^{h/2} T\,dy. \quad (5)$$

u and v are the velocity components in x and y directions and p and T are the hydrodynamics pressure and the temperature respectively.
The boundary conditions for the equations (1) and (2) are

When $y = 0$, $\frac{\partial u}{\partial y} = 0$ at $y = \frac{h}{2}$, $u = U$ $v_{h/2} = \frac{U}{2}\frac{dh}{dx} + \frac{V}{2}$ and $v_0 = 0$

Integrating equation (1) using the boundary conditions mentioned above, one may get

$$\bar{u} = 1 + \frac{\bar{f}}{\bar{h}^{(2n+1)/n}}\bar{s}. \quad -\infty < x \le x_2 \quad (6)$$

Where $\bar{s} = 2^{2+\frac{1}{n}}\left(\frac{2n+1}{n+1}\right)\left(\left(\bar{y}\right)^{1+\frac{1}{n}} - \left(\frac{\bar{h}}{2}\right)^{1+\frac{1}{n}}\right).$

Integrating the above continuity equation (2) using the conditions (6) and $\frac{dp_1}{dx} = 0$ at $x = -x_1$ and $h = h_1$, one can get in dimensionless scheme

$$\frac{d\bar{p}_1}{d\bar{x}} = \frac{\bar{m}_0\bar{E}}{\bar{h}^{2n+1}}\bar{f}^n. \quad -\infty < \bar{x} \le -\bar{x}_1 \quad (7)$$

$$\frac{d\bar{p}_2}{d\bar{x}} = -\frac{\bar{m}_0\bar{E}}{\bar{h}^{2n+1}}\bar{g}^n. \quad -\bar{x}_1 \le \bar{x} \le \bar{x}_2 \quad (8)$$

$$\bar{x} = x/\sqrt{2Rh_0};\ \bar{y} = y/h_0;\ \bar{h} = h/h_0;\ \bar{p} = \alpha p;\ \bar{g} = -\bar{f};\ \bar{E} = e^{\bar{p}+\left(\bar{T}_0/\bar{T}_m\right)};\ \bar{m} = 2mc_n\alpha.$$

$$\bar{f} = \bar{x}^2 - \bar{x}_1^{\,2} + 2q\left(\bar{x} + \bar{x}_1\right); \quad c_n = \left(\frac{2(2n+1)}{n}\right)^n \sqrt{\frac{2R}{h_0}}\left(\frac{U}{h_0}\right)^n; \quad \bar{T} = \beta T; \quad etc.$$

The energy equation for the one dimensional flow case may be assumed to be

$$k\frac{\partial^2 T}{\partial y^2} + \tau\frac{\partial u}{\partial y} = \rho c u \frac{dT_m}{dx}. \qquad (9)$$

Where k is the heat conduction of the fluid and is assumed to be constant.

Assuming, at $y = \frac{h}{2}$, $\frac{\partial T}{\partial y} = 0$; and at $y = 0$, $T = T_{01}$.

This above equation (10) is solved under boundary conditions mentioned above and is obtained with dimensionless scheme

$$\bar{T}_1 = \bar{T}_{01} + 6\bar{\xi}\frac{d\bar{T}_{m_1}}{d\bar{x}}\left(\left(\bar{y}^2 - \bar{h}\bar{y}\right) + \frac{\bar{l}\bar{f}}{\bar{h}^{\frac{2n+1}{n}}}\right) - \frac{\bar{m}_0\bar{E}\bar{f}^{n+1}\bar{\gamma}}{\bar{h}^{\frac{2n^2+3n+1}{n}}}\bar{t}. \quad -\infty < \bar{x} \le -\bar{x}_1 \qquad (10)$$

$$\bar{T}_2 = \bar{T}_{01} + 6\bar{\xi}\frac{d\bar{T}_{m_2}}{d\bar{x}}\left(\left(\bar{y}^2 - \bar{h}\bar{y}\right) - \frac{\bar{l}\bar{g}}{\bar{h}^{\frac{2n+1}{n}}}\right) - \frac{\bar{m}_0\bar{E}\bar{g}^{n+1}\bar{\gamma}}{\bar{h}^{\frac{2n^2+3n+1}{n}}}\bar{t}. \quad -\bar{x}_1 \le \bar{x} \le \bar{x}_2 \qquad (11)$$

Where $\bar{l} = 2^{2+\frac{1}{n}}\left(\frac{2n+1}{n+1}\right)\left(\left(\frac{n^2}{(3n+1)(2n+1)}\right)(\bar{y})^{3+\frac{1}{n}} - \left(\frac{\bar{h}}{2}\right)^{1+\frac{1}{n}}\frac{\bar{y}^2}{2} + \frac{n+1}{2n+1}\left(\frac{\bar{h}}{2}\right)^{2+\frac{1}{n}}\bar{y}\right)$

$\bar{t} = 2^{1+\frac{1}{n}}\left(\left(\frac{n}{3n+1}\right)(\bar{y})^{3+\frac{1}{n}} - \left(\frac{\bar{h}}{2}\right)^{2+\frac{1}{n}}\bar{y}\right)$; $\bar{y} = \frac{y}{h_0}$; $\bar{\gamma} = \frac{\beta U h_0}{k\alpha}\sqrt{\frac{h_0}{2R}}$;

Using the dimensionless scheme, the mean temperature T_{m_1}, as given in (5), can be calculated as

$$\frac{d\bar{T}_{m_1}}{d\bar{x}} = \left(\bar{T}_{m_1} - \bar{T}_{01} - \frac{b_n\bar{m}_0\bar{E}\bar{f}^{n+1}\bar{\gamma}}{\bar{h}^{2n}}\right) \Big/ \left(\zeta\left(a_n\bar{f}\bar{h} - \bar{h}^2\right)\right). \quad -\infty < \bar{x} \le -\bar{x}_1 \qquad (12)$$

$$\frac{d\bar{T}_{m_2}}{d\bar{x}} = \left(\bar{T}_{m_2} - \bar{T}_{01} - \frac{b_n\bar{m}_0\bar{E}\bar{g}^{n+1}\bar{\gamma}}{\bar{h}^{2n}}\right) \Big/ \left(\zeta\left(-a_n\bar{g}\bar{h} - \bar{h}^2\right)\right). \quad -\bar{x}_1 \le \bar{x} \le \bar{x}_2 \qquad (13)$$

Where $a_n = \left(\frac{18n^3+31n^2+15n+2}{2(n+1)(3n+1)(4n+1)}\right)$; $b_n = \left(\frac{10n^2+7n+1}{8(3n+1)(4n+1)}\right)$; $\zeta = \frac{\rho c}{k\sqrt{2Rh_0}}\frac{Uh_0^{\,2}}{12}$.

The normal load is given by

$$w_y = \int_{-\infty}^{x_2} p\,dx \qquad (14)$$

The dimensionless load $\overline{w_y} = \dfrac{W\alpha}{\sqrt{2Rh_0}}$ is given by

$$\overline{w_y} = \int_{-\infty}^{\overline{x_2}} \bar{x} \frac{d\bar{p}}{d\bar{x}} d\bar{x} \tag{15}$$

The tangential load is given [22] by

$$w_x = -2\int_{h_1}^{h_2} p\,dh = -2h_0 \int_{-\infty}^{x_2} x^2 \frac{dp}{dx} dx \tag{16}$$

The dimensionless load $\overline{w_x} = \dfrac{W_x\alpha}{2h_0}$ is given by

$$\overline{w_x} = \int_{-\infty}^{\overline{x_2}} \bar{x}^2 \frac{d\bar{p}}{d\bar{x}} d\bar{x} \tag{17}$$

The load $\overline{W}$ is calculated by

$$\overline{W} = \sqrt{\overline{w}_x^2 + \overline{w}_y^2} \tag{18}$$

the surface traction force T_F , obtained from the integration of shear stress τ over the entire length , may be written as

$$T_{Fh} = \int_{-\infty}^{x_2} \left(\frac{h}{2} \left(\frac{dp}{dx} \right) \right) dx \tag{19}$$

Then, the dimensionless traction may be written as

$$\overline{T_{Fh}} = \int_{-\infty}^{\overline{x_2}} \bar{h} \left(\frac{d\bar{p}}{d\bar{x}} \right) d\bar{x} \; ; \tag{20}$$

Finally, one can get the consistency expression in the form

$$\bar{m} = \overline{m_0}\, \bar{E} \, . \tag{21}$$

III. RESULT AND DISCUSSION

Calculation for a semi analytical solution of the Reynolds equations (7,8) and the heat energy equations(12,13) is done using the values below:

U = 4 m/s; R = 0.03 m; -0.09 < q < 0.09; 0.4 $\leq$ n $\leq$ 1.15; $\overline{T_{01}}$ = 8; $\overline{T_0}$ = 3; $\bar{\gamma}$ = 4; h_0 = 6 x 10^{-5} m;

α = 6 x10^{-8} pa^{-1} m^2

3.1 Pressure Profile –

Figures 2 and 3 show the distribution of pressure $\bar{p}$ is a function of U and 'n'. In figure 2 it could be seen the pressure profile $\bar{p}$ increases mostly with rolling ratio U for different n. In figure 3 it could be seen that $\bar{p}$ increases with different with fixed n. This module was displayed by Hajishafiee et al. [23] and Tobais Hultqvist et al [24].

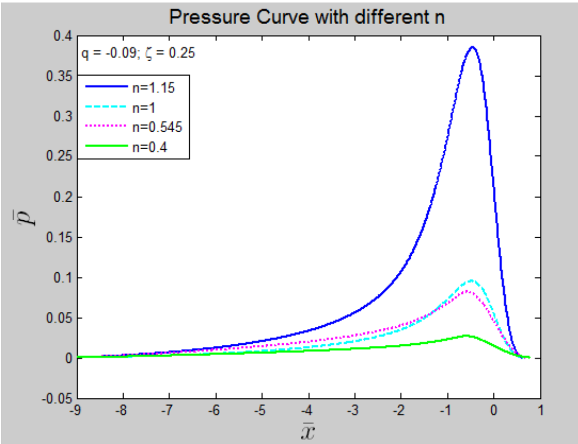

Fig 2: $\bar{p}$ against $\bar{x}$

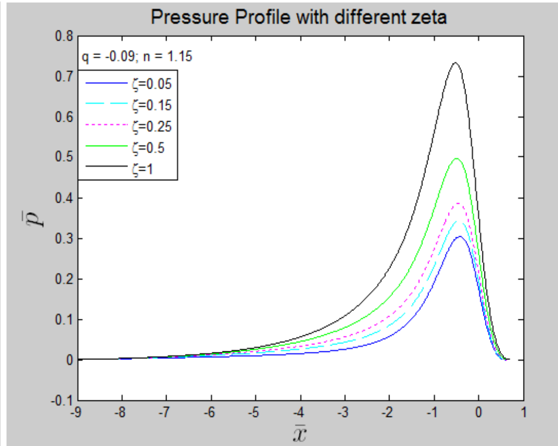

Fig 3: $\bar{p}$ against $\bar{x}$

3.2 Temperature Profile –

Figures 4 and 5 show the mean temperature $\overline{T_m}$ for various values of n with fixed ζ. The increase in mean temperature $\overline{T_m}$ with n shows that the temperature for dilatants fluid is higher than Newtonian and pseudo plastic fluid. Qualitatively, the mean temperature $\overline{T_m}$ against $\bar{x}$ is similar to that of the temperature profile received by Prasad et al. [21], the mean temperature $\overline{T_m}$ increase with q as per figure 5. From this it could be learnt that sliding temperature is higher than pure rolling. Further, it could be marked that the mean temperature $\overline{T_m}$ when 0 refer to the case without convection in Fig 4.

The increase in n hints an increase in effective viscosity [25]. Figures 6 and 7 show the two dimensional temperature distribution in $\bar{x}$ and $\bar{y}$ plane. ζ is almost zero and at this cause the figure 6 is drawn without convection. Whereas, figure 7 has the absolute distribution of temperature with convection and conduction.

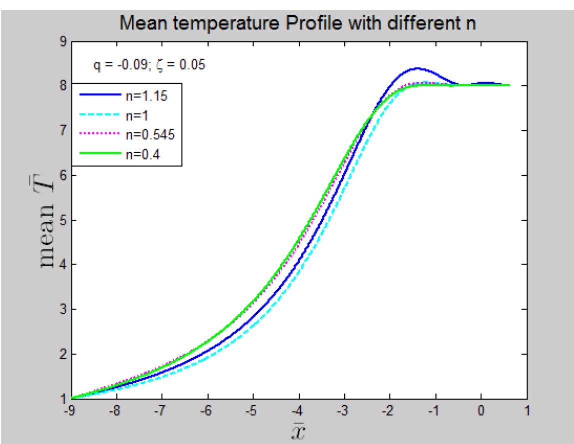

Fig 4: Mean $\bar{T}$ against $\bar{x}$

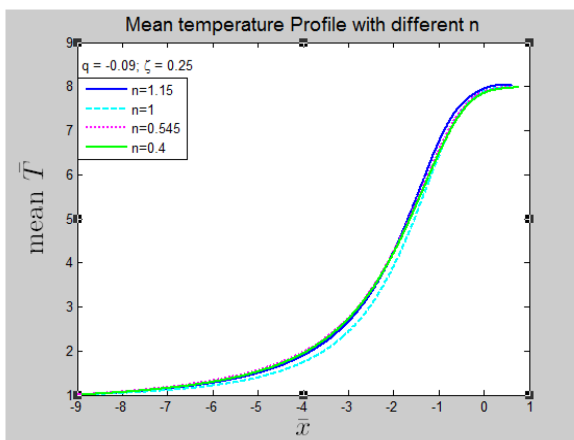

Fig 5: Mean $\bar{T}$ against $\bar{x}$

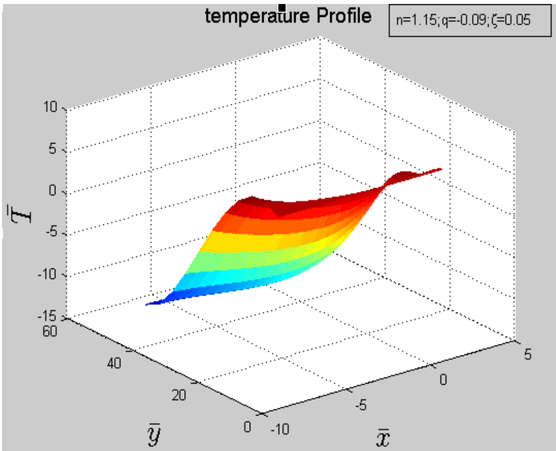

Fig 6: $\bar{T}$ against ($\bar{x}$ & $\bar{y}$)

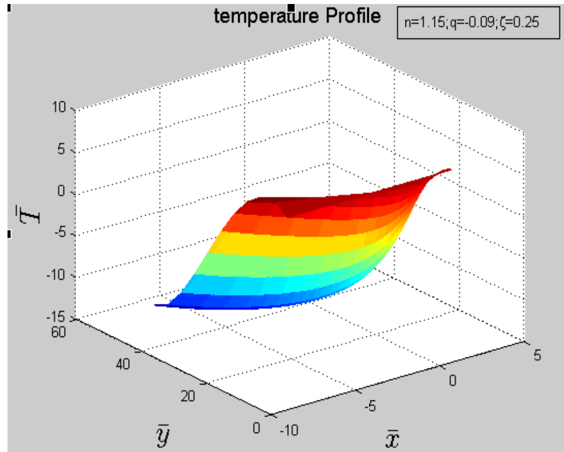

Fig 7: $\bar{T}$ against ($\bar{x}$ & $\bar{y}$)

3.3 Velocity Profile –

For constant values of q and n, the velocity distribution at various values of $\bar{x}$ between $\bar{x}$ =-9 and $\bar{x}$ =-0.6 is bestowed. Here, the velocity upsurges with $\bar{y}$, as the figure 8, shows, and this is similar to the work by Lorenzo Fusi[26]. As shown in figure 3 the velocity remains fixed when pressure peak is $\bar{x}$ =-0.6. The complete distribution of velocity with convection and conduction is shown figure 9.

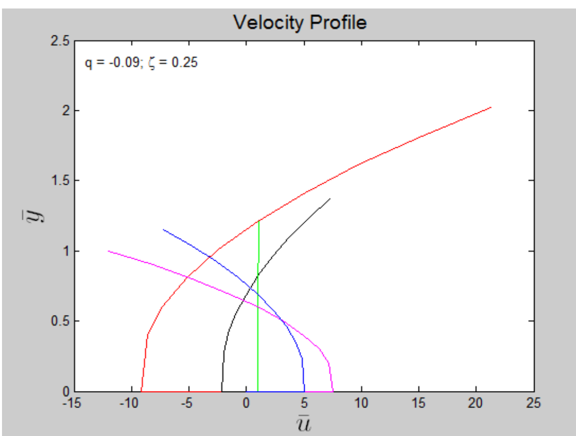

Fig 8: $\bar{y}$ against $\bar{u}$

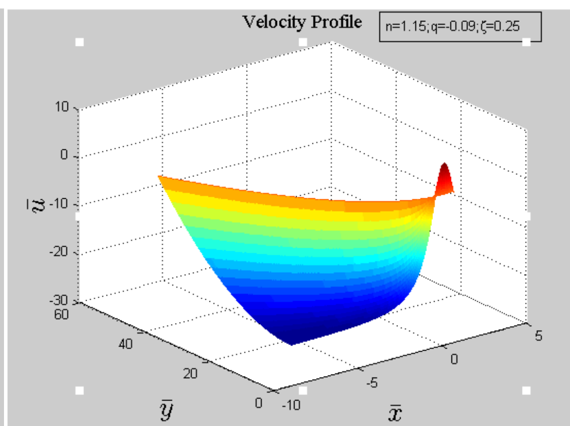

Fig 9: $\bar{u}$ against ($\bar{x}$ & $\bar{y}$)

3.4 Consistency Profile –

The lubricant consistency and its change in $\bar{m}$ with $\bar{p}$ and mean temperature $\overline{T_m}$ is the main subject of this article and it is clearly shown in the figures below. From figure 10 to 12, it is clear that the overall consistency changes with $\bar{x}$ for different n and different q and. It specifies the supremacy of pressure over the temperature for value below 0.1 and vice versa for ζ value 0.1 and above. So, the consistency variation with pressure and temperature is well justified [27,28].

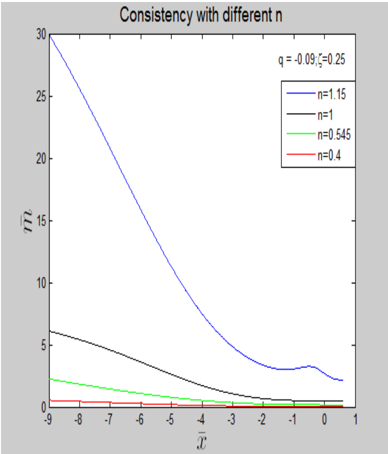

Fig 10: $\overline{m}$ against $\overline{x}$

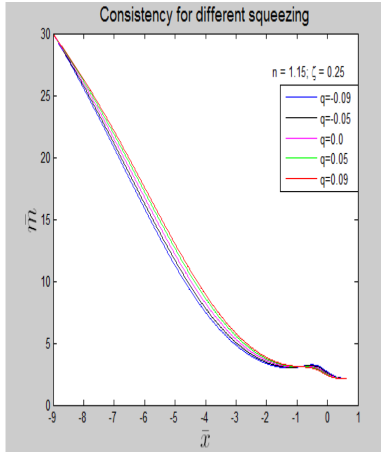

Fig 11: $\overline{m}$ against $\overline{x}$

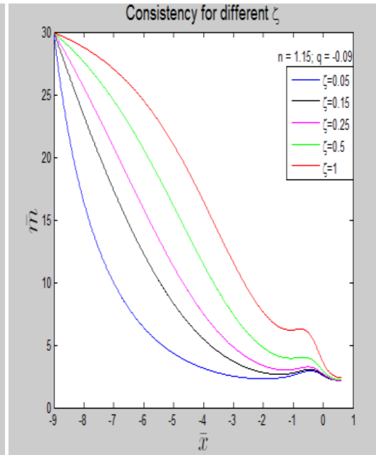

Fig 12: $\overline{m}$ against $\overline{x}$

3.5 Load and Traction –

Here, the table 1 represents the eccentric features of bearings namely the load $\overline{w}$ and the traction force $\overline{T_F}$ with different n and q values. Reading the table shows that both $\overline{w}$ and $\overline{T_F}$ increase with n and this is correlation with the earlier findings stated in [29]. Figures 13 to 15 denote load, traction, coefficient of traction against $\overline{x}$ and figure 16 shows the traction fore against normal load $\overline{W_y}$.

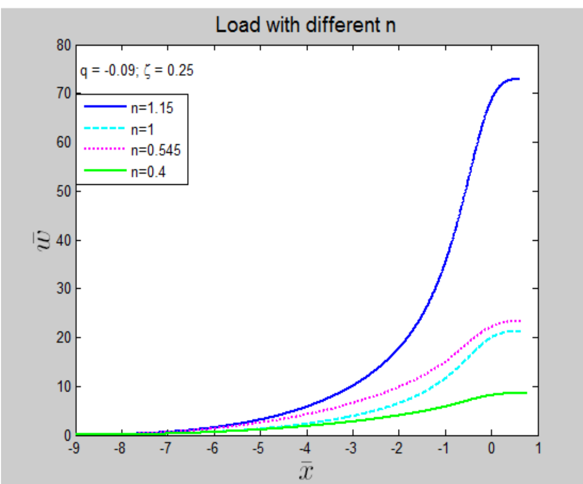

Fig 13: $\overline{w}$ against $\overline{x}$

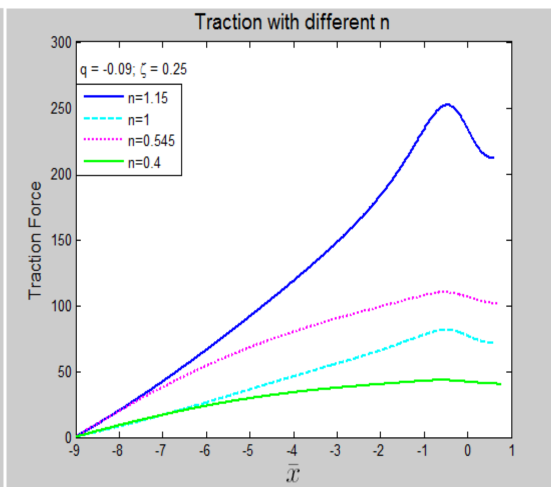

Fig 14: $\overline{T_F}$ against $\overline{x}$

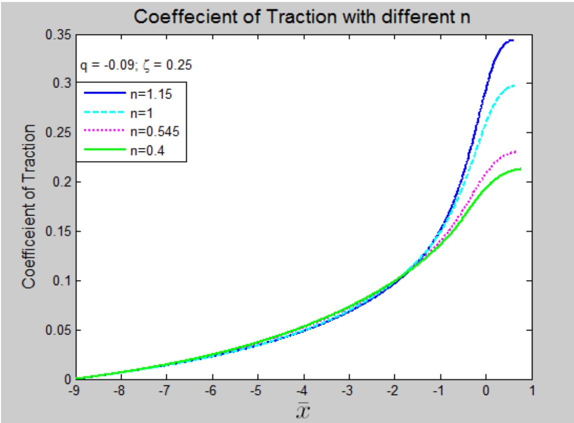

Fig 15: Co-efficient of $\overline{T_F}$ against $\bar{x}$

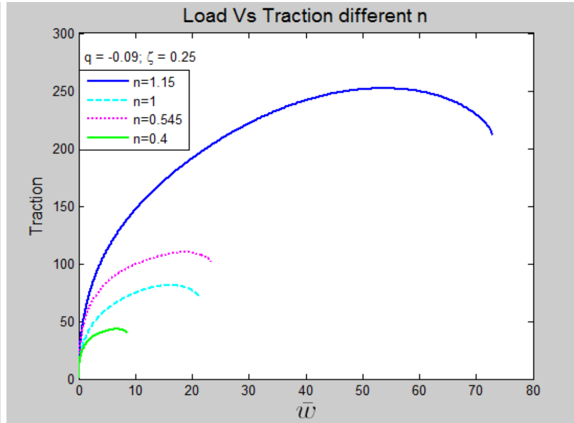

Fig 16: $\overline{T_F}$ against $\bar{w}$

Table -1 Load and Traction

n/ m_0	q=-0.09	q=-0.05	q=0.00	q=0.05	q=0.09
			x_1 **values**		
1.15/0.56	0.457460	0.484745	0.520866	0.558701	0.590000
1.00/0.75	0.477936	0.506334	0.543404	0.582658	0.615506
0.545/86.0	0.529518	0.562186	0.610295	0.667080	0.702344
0.40/128.0	0.596048	0.625888	0.665662	0.714949	0.749860
			x_2 **values**		
1.15/0.56	0.637460	0.584745	0.520866	0.458701	0.410000
1.00/0.75	0.657936	0.606334	0.543404	0.482658	0.435506
0.545/86.0	0.709518	0.662186	0.610295	0.567080	0.522344
0.40/128.0	0.776048	0.725888	0.665662	0.614949	0.569860
			Normal load		
1.15/0.56	0.728287	0.697383	0.661080	0.626262	0.599713
1.00/0.75	0.211555	0.206124	0.199348	0.192612	0.187270
0.545/86.0	0.233583	0.234338	0.235542	0.237062	0.236323
0.40/128.0	0.085741	0.086481	0.087233	0.087964	0.088366
			Traction		
1.15/0.56	2.116632	2.110030	2.096998	2.080945	2.066434
1.00/0.75	0.711910	0.714393	0.715818	0.715251	0.713533
0.545/86.0	1.013203	1.032708	1.052576	1.067242	1.080937
0.40/128.0	0.402739	0.413053	0.424604	0.434258	0.441572
			Coefficient of Traction		
1.15/0.56	2.906316	3.025641	3.172077	3.322802	3.445702
1.00/0.75	3.365124	3.465844	3.590789	3.713430	3.810186
0.545/86.0	4.337666	4.406923	4.468749	4.501953	4.573987
0.40/128.0	4.697139	4.776235	4.867469	4.936783	4.997085

IV.CONCLUSION

The problem attempts to study the thermal effects in hydrodynamic lubrication of roller bearings using incompressible power law fluid under adiabatic boundaries. The Reynolds and the thermal energy equations which are functions of consistency $\overline{m}$ and $\overline{u}$ and the consistency index n are obtained and solved semi analytically for pressure $\overline{p}$ and the mean temperature $\overline{T_m}$. The following are the inferences:

(i) The pressure increases significantly with n and ζ .

(ii) The sliding temperature is higher when compared to pure rolling.

(iii) The temperature is subjected to bring down the load carrying capacity of the system..

(iv) The load and traction rises with 'n' and q.

(v) The traction at lower surface is more because of high speed at lower surface than the upper surface.

(vi) The velocity of the lower surface is high resulting in the move of the velocity profile above the x- axis.

(vii) The mean film temperature upsurges considerably with n and ζ . So it is mandatory to treat the consistency $\overline{m}$ of the power law fluid to differ with temperature and pressure.

(viii) In the inlet domain, the effect of the peclet (ζ) number is more.

REFERENCES

[1] Dawson P H, "Effect of metallic contact on the pitting of lubricated rolling surfaces", J Mech Eng. Sci., 4(1):16–21, 1962.

[2] Liu JY, TallianTE, McCool JI, "Dependence of bearing fatigue life on film thickness to surface roughness ratio", ASLE Trans., 18:144–52, 1975.

[3] Skurka J, "Elasto hydrodynamic lubrication of roller bearings", Trans. ASME., J Lubr. Tech., 92(2):281–91, 1970.

[4] Danner CH, "Fatigue life of tapered roller bearings under minimum lubricant film", ASLE Trans., 13(4):241–50, 1970.

[5] Wilson AR, "The relative thickness of grease and oil films in rolling bearings", Proc. Inst. Mech Eng., 193:185–92, 1979.

[6] Heemskerk RS, Vermeiren KN, Dolfsma H, "Measurement of lubrication condition in rolling element bearings", ASLE Trans., 24:519–27, 1982.

[7] Leenders P, Houpert L, "Study of the lubricant film in rolling bearing; effects of roughness", Tribol. Ser., 11:629–38, 1987.

[8] Wardle FP, Jacobson B, Dolfsma H, Hoglund E, Jonsson U, "The effect of refrigerants on the lubrication of rolling element bearings used in screw compressors", In Int. compressor engineering conference, Purdue University, p. 523–34, 1992.

[9] Jacobson B, "Lubrication of screw compressor bearings in the presence of refrigerants", In International compressor engineering conference, Purdue University, p. 115–20, 1994.

[10] Franke E, Poll G, "Service life and lubrication conditions of different grease types in high-speed rolling bearings", Lubrication at frontier, Elsevier, p. 601–8, 1999.

[11] Lugt PM, "A review on grease lubrication in rolling bearings", Tribol Trans., 52: 470–80, 2009.

[12] Murer S, Bogard F, Rasolofondraibe L, Pottier B, Marconnet P, "Determination of loads transmitted by rolling elements in a roller bearing using capacitive probes: finite element validation", Mech Syst. Signal Process, 54–55:306–13, 2015.

[13] Schnabel S, Marklund P, Minami I, Larsson R," Monitoring of running-in of an EHLcontact using contact impedance", Tribol. Lett., 63:35, 2016.

[14] Jablonka K, Glovnea R, Bongaerts J. "Evaluation of EHD films by electrical capacitance", J Phys. D Appl. Phys., 45:385301, 2012.

[15] Lugt PM, "Grease lubrication in rolling bearings", Wiley, 2013.

[16] Dowson D, "The relationship between steady state wear rate and theoretical film thickness in metal-on-metal total replacement hip joints", Ins. of Tribology, School of Mech. Engg., Leeds, LS29JT.

[17] Cann PM, "Starvation and reflow in a grease-lubricated elasto hydrodynamic contact", Tribol. Trans., 39:698–704, 1996.

[18] Cann PM, "Starved grease lubrication of rolling contacts", Tribol. Trans., 42:867–73, 1999.

[19] Hurley S, Cann PM, Spikes HA, "Lubrication and reflow properties of thermally aged greases", Tribol. Trans., 43:221–8, 2000.

[20] Couronné I, Vergne P, Mazuyer D, Truong-Dinh N, Girodin D, "Effects of grease composition and structure on film thickness in rolling contact", Tribol. Trans., 46:31–6, 2003.

[21] Dhaneshwar Prasad and Venkata Subrahmanyam Sajja," Non-Newtonian Lubrication of Asymmetric Rollers with Thermal and Inertia Effects", Tribology Trans., 59:818-830, 2016.

[22] Prasad D and Punyatma Sing, Prawal Sinha, "Thermal and squeezing effects in Non-Newtonian fluid film lubrication of rollers", Wear, 119:175-190, 1987.

[23] A.Hajishafiee, A Kadiric, S. Ioannides and D. Dini, "A coupled finite volume CFD solver for two dimensional EHL problems with particular application to rolling element bearings", Tribology int., 109: 258-273, 2017.

[24] Tobias Hultqvista, Mohammad Shirzadegan, Aleks Vrcek, Yannick Baubet, Braham Prakash, Pär Marklund, Roland Larsson, "Elasto hydrodynamic lubrication for the finite line contact under transient loading conditions", Tribology Int., 127:489-99, 2018.

[25] Dhaneshwar Prasad and Venkata Subrahmanyam Sajja, "Thermal Effect in non--Newtonian Lubrication of Asymmetric Rollers Under Adiabatic and Isothhermal Boundaries" , Int. J. Chem. Sci., 14(3), 1641-1656, ISSN 0972-768X, 2016.

[26] Lorenzo Fusi, "Two-dimensional thin-film flow of an incompressible inhomogeneous fluid in a channel", J of Non-Newtonian Fluid Mech., 260: 87-100, 2018.

[27] G.E.Morales-Espejel, P.M.Lugt, H.R.Pasaribu H.Cen," Film thickness in grease lubricated slow rotating rolling bearings", Tribology Int., 74:7-19, 2014.

[28] Wang Li-li, Lu Chang-hou, "The effect of viscosity on the cavitation characteristics of high speed sleeve bearing", J. of Hydrodynamics, 27(3):367-72, 2015.

[29] P. Sinha and D. Prasad," Lubrication of rollers by power law fluids considering consistency variation with pressure and temperature", ActaMechanica, 111: 223-239, 1995.